In Vivo Assessment of Absolute Perfusion and Intracapillary Blood Volume in the Murine Myocardium by Spin Labeling Magnetic Resonance Imaging

Jörg U. G. Streif,[1*] Matthias Nahrendorf,[2] Karl-Heinz Hiller,[1] Christiane Waller,[2] Frank Wiesmann,[2] Eberhard Rommel,[1] Axel Haase,[1] Wolfgang R. Bauer[2]

The absolute perfusion and the intracapillary or regional blood volume (RBV) in murine myocardium were assessed in vivo by spin labeling magnetic resonance imaging. Pixel-based perfusion and RBV maps were calculated at a pixel resolution of 469 × 469 μm and a slice thickness of 2 mm. The T_1 imaging module was a segmented inversion recovery snapshot fast low angle shot sequence with velocity compensation in all three gradient directions. The group average myocardial perfusion at baseline was determined to be 701 ± 53 mL (100 g · min)$^{-1}$ for anesthesia with isoflurane (N = 11) at a mean heart rate (HR) of 455 ± 10 beats per minute (bpm). This value is in good agreement with perfusion values determined by invasive microspheres examinations. For i.v. administration of the anesthetic Propofol, the baseline perfusion decreased to 383 ± 40 mL (100 g · min)$^{-1}$ (N = 17, P < 0.05 versus. isoflurane) at a mean heart rate of 261 ± 13 bpm (P < 0.05 versus isoflurane). In addition, six mice with myocardial infarction were studied under isoflurane anesthesia (HR 397 ± 7 bpm). The perfusion maps showed a clear decrease of the perfusion in the infarcted area. The perfusion in the remote myocardium decreased significantly to 476 ± 81 mL (100 g · min)$^{-1}$ (P < 0.05 versus sham). Regarding the regional blood volume, a mean value of 11.8 ± 0.8 vol % was determined for healthy murine myocardium under anesthesia with Propofol (N = 4, HR 233 ± 17 bpm). In total, the presented techniques provide noninvasive in vivo assessment of the perfusion and the regional blood volume in the murine myocardium for the first time and seem to be promising tools for the characterization of mouse models in cardiovascular research. Magn Reson Med 53:584–592, 2005. © 2005 Wiley-Liss, Inc.

Key words: MRI; mice; myocardium; spin labeling; perfusion; intracapillary blood volume; anesthesia; myocardial infarction

Over the past decade, the mouse animal model has become an essential part of medical basic research. This is due to the high degree of similarity between the mouse and the human genomes of about 97% (1) and the resulting high relevance of mouse animal studies for human basic research. Regarding cardiovascular research, magnetic resonance imaging (MRI) provides noninvasive and accurate assessment of cardiac structure and function (2). Since the viability and the capability of the myocardium are strongly influenced by its microcirculation, a full characterization of the myocardium requires a quantification of parameters such as the perfusion and the intracapillary or regional blood volume (RBV). In particular, perfusion is of paramount importance as a physiologic parameter, since it strongly determines the function of organs and the severity of many diseases.

Heart diseases involving ventricular dysfunction and hypertrophy show significant alterations of the myocardial perfusion and transgenic mouse models may be well suited to elucidate the underlying fundamental mechanisms.

For the assessment of cardiac perfusion in mice, only a few methods have been presented to date. One possible approach is the quantification of the coronary flow in the isolated mouse heart by ultrasonic flow probes (3). The injection of labeled microspheres has also been applied to quantify the perfusion in murine myocardium (4,5). However, an important drawback of these ex vivo techniques is their invasiveness, which inhibits serial measurements in the same animal. This is a substantial limitation, since the full characterization of the remodeling after a myocardial infarction requires follow-up studies at different time points. In addition, the spatial resolution of microspheres examinations is limited, since a minimum number of microspheres is required in tissue specimens to obtain a sufficient accuracy (6). The cited method using ultrasonic flow probes provides no spatial resolution. As a consequence, these methods are not suitable to characterize the local consequences of diseases such as myocardial infarction (MI).

One possible approach to assess perfusion with MRI is contrast-enhanced first pass perfusion imaging (7). The basic principle is the tracking of the signal intensity change after the i.v. administration of a contrast agent. The analysis of the first pass of the contrast agent through the selected region of interest (ROI) provides information about the perfusion and the regional blood volume in this area.

Although this techniqe allows absolute quantification in principle (8), its reported usage in mice is currently confined to the relative assessment of perfusion changes in mouse hindlimbs after application of a vascular growth factor (9). In addition, contrast-enhanced MRI was used to study perfusion defects in murine myocardium (10). However, relative quantification of perfusion results in limited comparability of results of different studies.

[1]Physikalisches Institut, Lehrstuhl für Experimentelle Physik V (Biophysik), Universität Würzburg, Am Hubland, Würzburg, Germany.

[2]Medizinische Universitätsklinik, Universität Würzburg, Josef-Schneider-Strasse, Würzburg, Germany.

Grant sponsor: Deutsche Forschungsgemeinschaft; Grant number: DFG, WI 1510; SFB 355 "Pathophysiologie der Herzinsuffizienz", Teilprojekte A1, A6, A8; and DFG, HA 1232/8–1; Graduiertenkolleg "NMR".

*Correspondence to: Jörg U. G. Streif, Physikalisches Institut, Lehrstuhl für Experimentelle Physik V (Biophysik), Universität Würzburg, Am Hubland, 97074 Würzburg, Germany. E-mail: joerg.streif@web.de

Received 5 August 2003; revised 5 August 2004; accepted 5 August 2004.

DOI 10.1002/mrm.20327

Published online in Wiley InterScience (www.interscience.wiley.com).

This work's approach is based on the magnetic spin labeling of endogenous water protons. Pulsed labeling was performed within the imaging plane (11). This method has been well reported in the literature: the linear dependency between the spin lattice relaxation rate $R1 = 1/T_1$ after slice-selective inversion and the coronary flow in the isolated cardioplegic rat heart was first described in Ref. (12). Subsequently, the method was applied to the in vivo rat heart for the determination of basal myocardial perfusion (13) and for the quantification of perfusion in murine skeletal muscle (14). Substantial validation experiments were performed and range from local validation against measurements made with first pass perfusion imaging in the isolated rat heart (15) to comparison of in vivo data from the rat heart with microspheres examinations (16).

This approach provides quantification of regional blood volume by application of an intravascular contrast agent as well (17).

In this work we present a method for the absolute quantification of perfusion in murine myocardium in vivo that overcomes the cited limitations of competing techniques. This tool was then applied to study healthy and postinfarct mice and the impact of two different anesthetics. An additional objective was the quantification of regional blood volume in murine myocardium to further investigate the myocardial microcirculation.

METHODS

Quantification of Perfusion

The basic principle of the assessment of perfusion with spin labeling MRI is the combination of two different inversion recovery T_1 measurements with global and slice-selective spin inversion. The intrinsic relaxation of the selected tissue is observed with a global inversion. In the case of slice-selective inversion, only spins within the detection slice are affected by the inversion pulse; spins outside the detection slice rest in thermal equilibrium. If these spins enter the detection slice due to perfusion, they cause an apparent acceleration of the relaxation. The difference between the T_1 values $T_{1,\mathrm{sel}}$ (slice-selective inversion) and $T_{1,\mathrm{glob}}$ (global inversion) of the selected area therefore provides information about the perfusion in this area. The extraction of quantitative perfusion values requires the connection of the determined T_1 values with a tissue model such as the two-compartment model proposed in Ref. (18). Details of this entire procedure are published in Refs. (11–13,18), so we give only a brief summary of the essential points.

The tissue model describes tissue as consisting of two compartments, the intravascular capillary blood and the extravascular tissue. The arterial and venous systems are neglected. Two transport processes are taken into account: diffusion exchange between the two compartments and transport of spins from the arterial system to the capillary space due to perfusion.

It was shown in Ref. (13) that the absolute perfusion P can be estimated by

$$P = \frac{\lambda}{T_{1,\mathrm{blood}}} \cdot \left(\frac{T_{1,\mathrm{glob}}}{T_{1,\mathrm{sel}}} - 1 \right), \qquad [1]$$

where $T_{1,\mathrm{blood}}$ is the T_1 of capillary blood and λ denotes the blood–tissue partition coefficient for water defined as

$$\lambda = \frac{\text{quantity of water per gram tissue}}{\text{quantity of water per milliliter blood}}. \qquad [2]$$

This technique for the estimation of perfusion has been validated against measurements made with microspheres in prior works (16). In addition, a local validation of the same technique against measurements with first pass perfusion imaging was performed for the isolated rat heart (15).

Equation [1] provides information about the needed accuracy of the T_1 quantification for the assessment of myocardial perfusion with this technique. Assuming a $T_{1,\mathrm{glob}}$ of 1600 ms for murine myocardium, a $T_{1,\mathrm{blood}}$ of 1650 ms and a blood–tissue partition coefficient of 0.95 mL g^{-1} results in a $T_{1,\mathrm{sel}}$ of 1350 ms for a myocardial perfusion of 640 mL $(100\ g \cdot min)^{-1}$, a value that was determined in a microspheres study (5). Typical differences $T_{1,\mathrm{glob}} - T_{1,\mathrm{sel}}$ are therefore in the range of 250 ms in the murine myocardium (it is noted that all T_1 values are specified for a field strength of 7 T).

Quantification of the RBV

As shown in Ref. (17), a similar technique provides quantification of the regional blood volume RBV as well. In this case, the adminstration of an intravascular contrast agent is required and the relation

$$\mathrm{RBV} = \lambda \left(\frac{1/T^{\mathrm{ca}}_{1,\mathrm{sel}} - 1/T_{1,\mathrm{sel}}}{1/T^{\mathrm{ca}}_{1,\mathrm{blood}} - 1/T_{1,\mathrm{blood}}} \right) \qquad [3]$$

holds, where $T_{1,\mathrm{sel}}$ and $T^{\mathrm{ca}}_{1,\mathrm{sel}}$ are the tissue T_1 values for slice-selective inversion before and after the application of the contrast agent and $T_{1,\mathrm{blood}}$ and $T^{\mathrm{ca}}_{1,\mathrm{blood}}$ denote the T_1 of capillary blood before and after the application of the contrast agent. Equation [3] shows the needed accuracy of the T_1 quantification for the assessment of the RBV. Assuming a $T_{1,\mathrm{sel}}$ of 1350 ms, a $T_{1,\mathrm{blood}}$ of capillary blood of 1650 ms before the application of the contrast agent, a decrease in T_1 of blood of 1000 ms due to the contrast agent, and a blood–tissue partition coefficient of 0.95 mL g^{-1} results in a $T^{\mathrm{ca}}_{1,\mathrm{sel}}$ of 1192 ms. Typical differences $T_{1,\mathrm{sel}} - T^{\mathrm{ca}}_{1,\mathrm{sel}}$ are therefore in the range of 150 ms in murine myocardium.

It is also noteworthy that this technique for the quantification of the RBV provides an intrinsic perfusion correction and eliminates the potential overestimation of the RBV due to perfusion.

Hardware and MRI

All MR experiments were performed on a Bruker Biospec 70/20 scanner at 7.05 T. A dedicated gradient insert for microscopy imaging with a maximum gradient strength of 870 mT/m and a bore diameter of 60 mm was used.

The T_1 quantification was performed using an inversion recovery snapshot fast low angle shot (FLASH) sequence (19) as shown in Fig. 1. The basic principle is the tracking

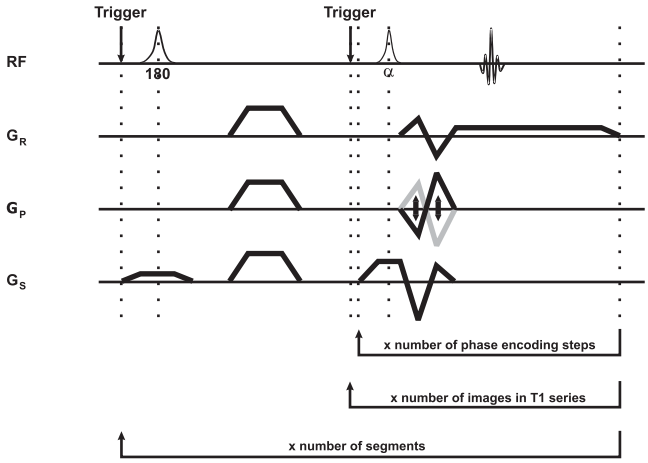

FIG. 1. The inversion recovery snapshot FLASH pulse sequence used for quantification of T_1 with a slice-selective inversion pulse. All imaging gradients are velocity-compensated in the first order and avoid phase accumulations due to constant velocity motion. A similar sequence without a slice gradient during the inversion pulse was used for the global measurements of T_1.

of the relaxation of the magnetization by a series of FLASH images after initial spin inversion.

To reduce motion artifacts, first-order velocity compensation was performed by rephasing gradients (20). Since this design avoided phase accumulations due to constant velocity motion, the images were not sensitive to velocity-induced artifacts such as signal loss due to intravoxel dephasing, blurring in read-direction, and misregistration in the phase encoding direction. However, the additional gradients resulted in an extension of the echo time TE by 280 μs. On the other hand, TE was reduced by detection of the center of each echo at 1/4 of the acquisition window. In total, this resulted in a TE of 1.5 ms and a repetition time TR of 2.6 ms. A flip angle between 3 and 5° was chosen for the experiments.

The image acquisition was electrocardiogram-(ECG)-gated to account for the periodic heart motion. Since minimal heart motion as well as maximum myocardial perfusion occurs during the diastole of the heart, the image acquisition was performed during this heart phase. At typical heart rates of about 450 beats per minute (bpm) the duration of diastole was about 80 ms. As a consequence for the given TR, a segmented image acquisition was mandatory.

Following the initial spin inversion with a adiabatic hyperbolic secant inversion pulse (duration 4 ms, bandwidth 2.4 kHz), 48 *k*-space segments were acquired to track the relaxation of the magnetization. Depending on the individual heart rate, the duration of this was about 7 s. With 32 *k*-space lines per segment and a final matrix size of 64 × 64, two cycles were required for one T_1 measurement with 48 images after the spin inversion. The field of view (FOV) was adjusted to 30 × 30 mm, the imaging slice thickness was 2 mm, and the radiofrequency (RF) excitation was performed with a sinc-shaped pulse with a duration of 500 μs.

For global spin inversion, considerations about the blood circulation time were mandatory. The blood volume in mice is about 5% of the body mass (21). Combining this with typical body masses and cardiac outputs given in Ref. (22) shows that the whole blood volume circulates once in about 4.5 s. Since this is in the range of the duration of the T_1 quantification, a proper spin inversion within the whole mouse is mandatory.

The size of the transmitting RF coil therefore has to be sufficiently large to ensure that the whole mouse is located in a region with sufficient homogeneity of the B_1 field. However, the region of interest where an estimation of the perfusion and the RBV is desired is usually only a part of the mouse such as the myocardium in this study. The need for a large coil during transmission thus results in a poor filling factor for detection of the MR signal. It is therefore advantageous to combine separate transmission and detection coils with separately adapted sizes. For this study, a dedicated coil combination was constructed. A RF resonator in birdcage design served as transmission coil (eight legs, inner diameter 32 mm, length 110 mm, linear drive). For detection of the MR signal, a surface coil with an adapted size for studies on the murine heart was constructed. Both coils were actively decoupled using PIN-diode switches. Further details are described in Ref. (23). Using this coil in combination with adiabatic hyperbolic secant inversion pulses (24) guaranteed exact spin inversion over the whole mouse and detection with high SNR. To guarantee a sufficient shim over the whole mouse, shimming was performed using the volume coil for transmission and for detection. Typical linewidths over the whole mouse were lower than the bandwidth of 2.4 kHz of the inversion pulse.

For slice-selective inversion, an optimization of the inversion slice thickness with respect to the imaging slice thickness was mandatory. This was performed in an experiment using a phantom tube with a diameter of 30 mm filled with Krebs–Henseleit buffer. For a constant imaging slice thickness of 2 mm, the inversion slice thickness was increased starting with 2 mm until no significant difference between $T_{1,\mathrm{sel}}$ and $T_{1,\mathrm{glob}}$ of the phantom occurred (data not shown). As a consequence, the inversion slice thickness was adjusted to 6 mm throughout.

Animal Handling and Experimental Protocol

All experiments were performed in accordance with the European guidelines for the care and the use of laboratory animals. In total, the study was performed on 34 female mice. A heating pad maintained normothermic conditions. For ECG gating, electrodes were positioned on the superior feet and connected to a homebuilt ECG trigger unit (25).

The experimental protocol started with the acquisition of scout images to localize the animal's heart. The detection slice for the T_1 measurement was positioned in a midventricular short axis view. T_1 measurements were performed as described with interleaved slice-selective and global inversion. To increase the SNR, 16 signal averages were performed. Depending on the individual heart rate, the duration of one perfusion experiment ranged from 30 to 40 min for a single slice.

A group of 11 healthy C57BL/6 mice (mean body mass 25.3 ± 0.9 g) was anesthetized by inhalation of isoflurane (Abbott GmbH, Wiesbaden, Germany). For initiation of

anesthesia, the isoflurane concentration was adjusted to 4.0 vol % and then lowered to 1.5 vol % during the measurement. The oxygen flow was adjusted to 1.5 L/min.

In addition, a second group of six C57BL/6 mice with MI was examined under the identical protocol. The mean body mass in this group was 28.4 ± 0.3 g. MI was induced by surgical ligation of the left anterior descending (LAD) coronary artery and MRI was performed 4 weeks postligation.

In a third group of 17 NMRI mice (mean body mass 24.1 ± 0.5 g), anesthesia was initiated by an intraperitoneal (i.p.) application of 100 mg kg^{-1} Propofol (AstraZeneca GmbH, Wedel, Germany) and maintained via an i.v. catheter in the tail vein at a constant dose of 20 mg $(kg\ h)^{-1}$. In addition, this group was orally intubated and ventilated by room air using a rodent ventilator (BAS-7025, FMI, Germany). The breathing volume was adjusted to 1.0 mL per breath at a frequency of 120 Hz. For this group, the ventilation was automatically stopped during the MR acquisition to examine the degree of respiratory motion artifacts with respect to the groups with isoflurane anesthesia. After the first cycle with interleaved global and slice-selective inversion for the assessment of the perfusion, a subgroup of 4 animals (mean body mass 23.5 ± 1.2 g) received a bolus of the contrast agent Gd-DTPA-albumin (0.7 μmol kg^{-1}) i.v. with subsequent restart of the MR protocol for quantification of the RBV. The contrast agent was synthesized by labeling pig serum albumin with Gd-DTPA as described in Ref. (26). Due to its high molecular weight, Gd-DTPA-albumin enhances relaxation only in the intravascular space.

Postprocessing

All postprocessing was performed using Interactive Data Language (Research Systems Inc., Boulder, CO). After zero filling to a matrix size of 128 × 128, a three-parameter least-squares fit of the equation

$$M(t) = A \cdot (1 - B \cdot e^{-t/T_1^*}) \qquad [4]$$

was applied for each image pixel to calculate T_1 from the image data. This fit procedure required exact knowledge of the timing of each image with respect to the inversion pulse. Monitoring of the sequence timing was accomplished with an external computer taking the end of the inversion pulse as the time origin. A χ^2 goodness-of-fit test was performed and fitted image pixels with $\chi^2 > 0.5$ were suppressed from further processing.

Due to saturation effects under the train of low-angle RF pulses, the fitted time constant T_1^* is not the desired spin-lattice relaxation time T_1. Corrections involving A and B have to be applied in order to calculate the true T_1 from T_1^* (27) by

$$T_1 = T_1^* \cdot \left(\frac{B}{A} - 1\right). \qquad [5]$$

These corrections were automatically performed during the processing.

Pixel-based quantitative perfusion and RBV maps were subsequently calculated by use of Eqs. [1] and [3] under the assumption of a blood–tissue partition coefficient λ of 0.95 mL/g in the myocardium (28).

Statistics

All values are reported as means ± SE mean (SEM). Analysis of variance between groups (ANOVA) was applied to test for significant variations. A significance level of $P < 0.05$ was considered statistically significant throughout.

RESULTS

Under anesthesia with isoflurane, the mean heart rate during MRI was 455 ± 10 bpm for healthy mice and 397 ± 7 bpm for mice with MI. Anesthesia with Propofol caused a lower mean heart rate of 261 ± 13 bpm.

Figure 2 shows representative data of mice that were anesthetized by inhalation of isoflurane. All measurements were performed in a midventricular short axis view. Figure 2a depicts the zoomed quantitative T_1 map after global spin inversion, where the blood inside the left ventricle (LV) and the myocardium appear as relatively homogeneous areas.

This behavior is altered for slice-selective spin inversion as shown in Fig. 2b. Here, the apparent acceleration of the relaxation due to perfusion results in lower T_1 values for the myocardium and—to a higher extent—for the blood inside the LV. Figure 2c depicts the zoomed quantitative perfusion map calculated by use of Eq. [1].

Figure 2d shows a representative perfusion map of a mouse with myocardial infarction that was anesthetized by isoflurane as well. The decrease of the perfusion in the infarcted anterolateral area (arrow) is clearly visible.

Figure 3 depicts representative maps from an animal under i.v. anesthesia with Propofol. To assess the degree of image artifacts due to the respiration motion, two subsequent global T_1 maps were acquired for one intubated animal anesthetized with Propofol. In this experiment, the ventilation was automatically stopped during the acquisition of the first global T_1 map and continued during the acquisition of the second global T_1 map. Figure 4 shows the calculated maps. To extract quantitative data, ROIs containing essentially the whole myocardium (healthy mice) or the remote myocardium (mice with MI) were manually selected excluding the regions that showed partial volume errors with the surrounding tissue.

Figure 5 summarizes the quantitative results for the perfusion. For comparison, the result of the microspheres examination (5) has been added to Fig. 5. The healthy mice showed a group average perfusion of 701 ± 53 mL $(100\ g \cdot min)^{-1}$ under anesthesia with isoflurane. The mean perfusion of the group with MI was 476 ± 81 mL $(100\ g \cdot min)^{-1}$ in the remote myocardium. Under anesthesia with Propofol, the mean perfusion was 383 ± 40 mL $(100\ g \cdot min)^{-1}$.

The group average regional blood volume in the myocardium was determined to be 16.9 ± 0.8 vol %.

T_1 of blood was individually quantified in the LV in T_1 maps with global spin inversion and resulted in a group average T_1 of 1609 ± 97 ms for healthy mice under anes-

thesia with isoflurane, 1767 ± 108 ms for mice with MI under isoflurane and 1684 ± 54 ms for healthy mice under adminstration of Propofol. The subgroup for which the RBV was quantified showed a basal group average T_1 of blood of 1847 ± 165 ms that decreased to 1235 ± 261 ms after administration of the contrast agent.

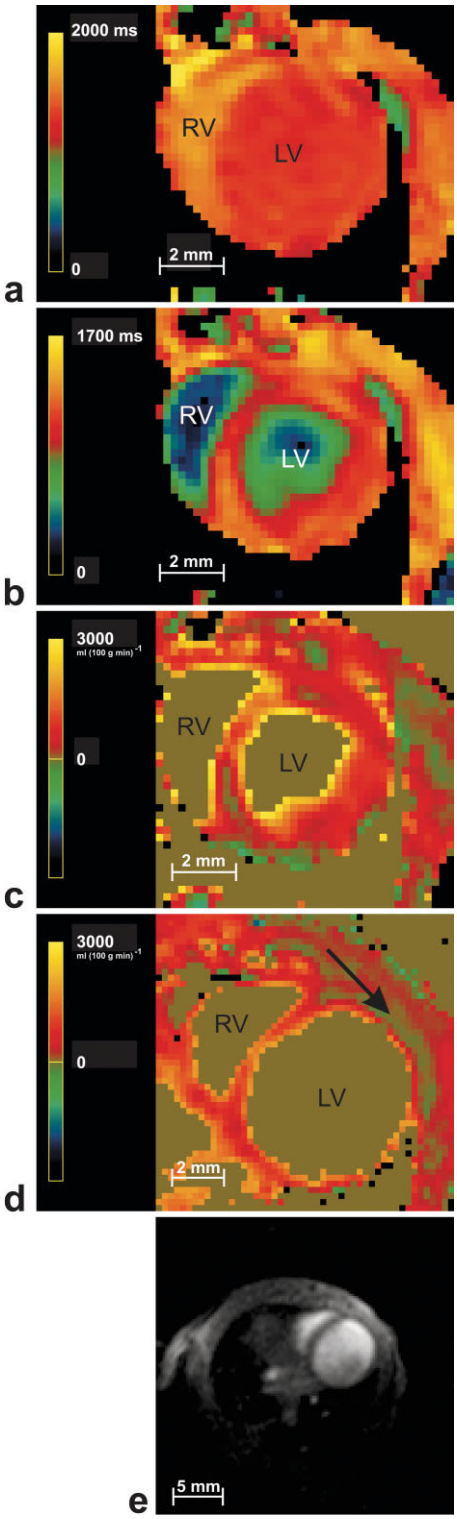

DISCUSSION AND CONCLUSION

We have been able to demonstrate that spin labeling MRI is a technique that is well suited for the in vivo quantification of the perfusion and the regional blood volume of murine myocardium. The method was based on the acquisition of T_1 maps with global and slice-selective inversion pulses and allowed the calculation of quantitative perfusion and regional blood volume maps at a single-pixel resolution of 469 × 469 μm and a slice thickness of 2 mm. Using this technique, the quantification of the perfusion is contrast-medium independent, whereas the assessment of the RBV requires the i.v. administration of an intravascular contrast agent.

Under anesthesia with isoflurane, a mean perfusion of 701 ± 53 mL (100 g · min)$^{-1}$ was determined for healthy murine myocardium. This value decreased to 383 ± 40 mL (100 g · min)$^{-1}$ for administration of Propofol.

Since no other method for the in vivo assessment of the absolute perfusion in the murine myocardium exists, a comparison of these results is only possible with results of invasive microspheres examinations.

In the first paper that studied the feasibility of radioactively labeled microspheres to assess murine hemodynamics (4), the blood flow to the heart was determined to be 6 ± 2% of the cardiac output (CO) in mice anesthetized with Avertin. In Ref. (4), the animals showed a mean heart rate of 459 ± 38 bpm; the mean CO was 17.3 ± 3.1 mL min^{-1}. The myocardial perfusion P can be calculated by P = %CO CO m_{heart}^{-1}. Unfortunately m_{heart} was not determined in Ref. (4). However, it was stated in Ref. (29) that the ratio between heart mass and body mass is about 5 mg g^{-1} for mice. Assuming a body mass of 25 g therefore results in a heart mass of 125 mg. In total, the combination of Refs. (4) and (29) results in a myocardial perfusion of 830 ± 317 mL (100 g · min)$^{-1}$. Currently, no information about the influence of anesthesia with Avertin on the myocardial perfusion is available from the literature.

A very recent study with fluorescently labeled microspheres determined a mean myocardial perfusion of 640 ± 40 mL (100 g · min)$^{-1}$ for healthy wild-type mice at a mean heart rate of 453 ± 21 bpm (5).

FIG. 2. Representative data from mice anesthetized by inhalation of isoflurane. Perfusion was assessed in the midventricular short axis view. The zoomed T_1 maps after global spin inversion (**a**) and after slice-selective spin inversion (**b**) are the basis for the calculation of a pixel-by-pixel quantitative perfusion map as shown in (**c**). Note the apparent acceleration of the relaxation in the myocardium and for blood inside the left (LV) and the right ventricle (RV) due to perfusion in (b). T_1 of blood was determined inside the left ventricle in (a). (**d**) shows the perfusion map of a mouse with myocardial infarction in the anterolateral area that was already visible with cine MRI. The perfusion in this area is clearly decreased with respect to the healthy myocardium (arrow). (For further illustration, some exemplary quantitative T_1 data are given for the particular mouse with MI depicted in (d): for identical regions located anterior (septal), T_1 was determined to be 1873 ± 13 ms (1930 ± 37 ms) after global spin inversion and 1796 ± 24 ms (1429 ± 39 ms) after slice-selective spin inversion, respectively.) Furthermore, it is noted that (c) and (d) were equally scaled. (**e**) depicts one representative source image from the T_1 data set after global spin inversion used as an input for the T_1 mapping algorithm.

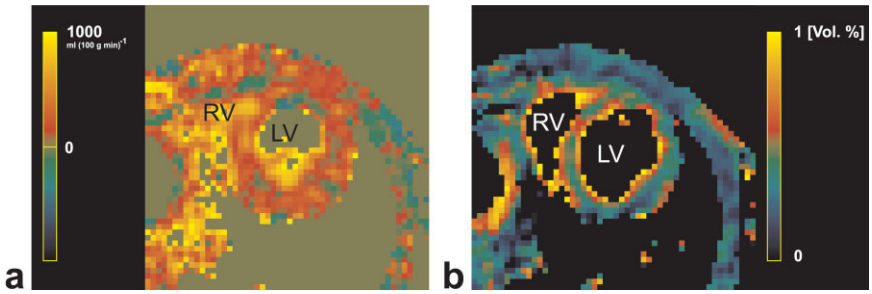

FIG. 3. Representative data from a mouse under i.v. administration of the anesthetic Propofol. (**a**) shows a zoomed perfusion map in a midventricular short axis view; (**b**) depicts the corresponding perfusion-corrected regional blood volume map with values given in vol %.

In this study, healthy animals under anesthesia with isoflurane showed basically identical heart rates with respect to the cited microspheres studies. The determined mean perfusion of 701 ± 53 mL $(100\ g \cdot min)^{-1}$ is within the bandwidth given by microspheres examinations. It should, however, be noted that this value is unlikely to reflect the true basal perfusion, since perfusion increases of up to 50% have been described during anesthesia with isoflurane (30). Moreover, it is to be noted that no validation against measurements made with microspheres was performed in this study.

For anesthesia with Propofol, the mean perfusion was about 46% lower than during anesthesia with isoflurane. It is noteworthy that the mean heart rate under Propofol decreased as well by a factor of 43% (due to the initial i.p. injection of Propofol). This suggests that the decreased perfusion under Propofol primarily reflects the lower heart rate under this anesthetic. In addition, Propofol does not show a vasodilatoric effect.

The self-breathing group under isoflurane showed no significant degree of respiratory motion artifacts with respect to the group where the ventilation was stopped during the MR acquisition. This missing influence of respiratory motion under isoflurane was already noted earlier in cine imaging and in high-resolution imaging of the coronary arteries of the mouse heart. A possible explanation is the low ratio of about 1:8 between the breathing rate and the heart rate for this anesthetic (31). In addition, the inspiration phase is very short with respect to the total breathing cycle. It has also been shown that serial averaging (16 signal averages in this study) further reduces respiratory artifacts (32). Furthermore, one could speculate that the motion of the heart due to breathing is relatively small compared to the thickness of the inversion slice of 6 mm used in this study.

Regarding the absence of significant respiratory artifacts, its easy regulation, and the fact that isoflurane produces physiologic heart rates and a very stable heart function during anesthesia (33), this anesthetic seems to be superior for studies where its vasodilatoric effect is of minor importance.

The baseline myocardial perfusion and regional blood volume showed a homogeneous distribution over the myocardium and no significant variations were detectable. This is not an inconsistency with recent studies that demonstrated the spatial heterogeneity of perfusion in the heart (34) since the spatial resolution in our study is not high enough to resolve the heterogeneous areas with typical sizes lower than 200 × 200 μm.

Regarding MI, the presented technique allowed the visualization and detection of infarcted areas that showed a reduced perfusion. The scar thickness for MI was determined by additional cine MRI to be 530 ± 4 μm. At an imaging resolution of 469 × 469 μm, the quantification of perfusion in the infarcted zones therefore suffers from substantial partial volume errors. Therefore, the determination of perfusion values in the infarcted areas was not possible. This limitation is of minor importance, since the remaining function and power of the heart are determined by the remote myocardium.

Here, the perfusion decreased significantly to 476 ± 81 mL $(100\ g \cdot min)^{-1}$. This represents the remodeling after MI and the presented results are consistent with findings in rats after MI (35). After MI, the remote myocardium hypertrophies (36). However, due to insufficient growth of capillaries, capillary density decreases (37), leading to reduced perfusion values in the remote myocardium when compared to healthy mice.

Beside the first noninvasive determination of the absolute perfusion in murine myocardium with MRI, we have been able to demonstrate the quantification of the regional blood volume in murine myocardium as well.

In our study, we determined a group average regional blood volume of 16.9 ± 0.8 vol % in healthy myocardium. This value was calculated under the assumption that the T_1 of blood is identical in the left ventricle and the capil-

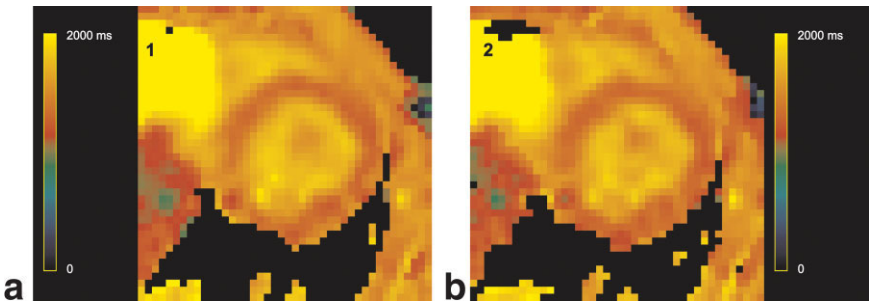

FIG. 4. Influence of respiratory motion on the image quality. The global T_1 map of (**a**) was acquired with continued respiration. The ventilation was stopped during the acquisition of the global T_1 map of (**b**).

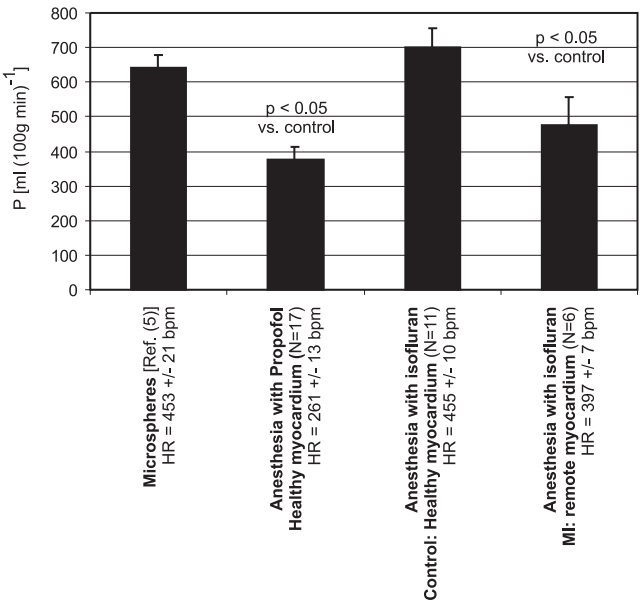

FIG. 5. Comparison of the quantitative group average perfusion for anesthesia by inhalation of isoflurane and i.v. administration of Propofol for healthy and postinfarct mice (HR = heart rate, bpm = beats per minute).

laries. However, this is not the case after the application of the contrast agent since the contrast agent distributes exclusively in the blood plasma. It has been shown in Ref. (17) that a corrected RBV_c can be calculated involving the hematocrit (hct) by $RBV_c = RBV \cdot \lambda \cdot (1 - hct_{LV})/(1 - hct_{capillaries}) \approx 0.7 \cdot RBV$. Performing this results in a RBV_c of 11.8 ± 0.8 vol %. Currently, no quantitative data are available in the literature for a comparison. The determined RBV_c shows a good agreement with the RBV of the rat heart determined with MRI (17) and other methods (38,39), which resulted in values between 10 and 13%.

A principal advantage of the presented in vivo techniques is their noninvasiveness. As a consequence, serial studies in the same animal are possible over long time periods. Due to the absolute quantification, the comparison of serial measurements at different time points or from animal to animal is easy and accurate.

One major limitation of the presented methods is the long acquisition times, which were necessary to obtain a sufficient SNR and a corresponding high accuracy of the T_1 quantification. With a duration of about 30 min for one perfusion quantification in a single slice, the time resolution of the presented technique is too small to monitor dynamic processes on smaller time scales.

Since the quantification of the RBV requires a baseline measurement (which provides the baseline perfusion as well) and a second cycle after the administration of the contrast agent, the total duration of a combined perfusion and RBV quantification is about 60 min for a single slice.

It should as well be noted that the presented technique requires a stable heart rate during the acquisition time. In addition, the spatial resolution is not sufficiently high to distinct perfusion differences across the heart wall such as differences between epi- and endocardial areas. The limited spatial resolution is as well an issue for the examination of infarcted zones with their reduced thickness of the heart wall.

In addition, the method suffers from disadvantageous statistical error propagation since the errors $\Delta T_{1,glob}$ and $\Delta T_{1,sel}$ of the measured T_1 values contribute as fractions $\Delta T_{1,glob}/(T_{1,glob} - T_{1,sel})$ and $\Delta T_{1,sel}/(T_{1,glob} - T_{1,sel})$ to the relative error of the perfusion. In our data, typical relative errors of the fit parameters A, B, and T_1^* (see Eq. [4]) are in the range of up to 3% per pixel. As a consequence, relative errors in the murine myocardial perfusion are in the range of up to 40% per pixel. The same disadvantageous behavior holds for the quantification of the RBV.

In the case of slice-selective IR T_1 measurements, considerations with respect to the profiles of the inversion pulse and the imaging pulses are mandatory. In the hypothetic ideal case, spins within the detection slice of the imaging pulses are completely inverted after the inversion pulse, whereas all other spins are not influenced by the inversion pulse. Imperfections in the real excitation pulses can cause two basic effects: (i) Inproper inversion within the detection slice leads to an apparent acceleration of the relaxation, i.e., a shorter $T_{1,sel}$ and therefore an overestimation of perfusion. (ii) Inversion of spins adjacent to the detection slice results in a longer $T_{1,sel}$ since perfusion transports inverted spins instead of equilibrium spins to the detection slice for a certain time interval after the inversion. This causes an underestimation of perfusion. In the pulse sequence used in this study, the spin inversion for global and slice-selective T_1 measurements was accomplished using adiabatic hyperbolic secant inversion pulses (24) with a duration of 4 ms. In the case of slice-selective inversion, the ratio between the inversion slice thickness and the detection slice thickness was adjusted to 3:1 to avoid an overestimation of perfusion. In a phantom study, no significant difference between $T_{1,sel}$ and $T_{1,glob}$ occurred for this ratio (data not shown).

For slice-selective inversion, it is as well important to discuss the duration of the T_1 measurement of about 7 s with respect to the recirculation time of blood in the mouse of about 4.5 s. Spins that have been initially inverted by the slice-selective inversion pulse enter and leave the detection slice due to perfusion. In principle, these spins could alter the measured acceleration of the T_1 relaxation if they reenter the detection slice (i) in a sufficiently high number and (ii) with a significant difference from being in thermal equilibrium. However, this is not the case since: (i) the selective inversion pulse is short (4 ms) and affects only spins in a small fraction of the mouse (inversion slice thickness 6 mm with respect to a total animal length of at least 70 mm). Regarding the topology of the vascular system, it is extremely unlikely that a significant number of initially inverted spins even reaches the detection slice after the first recirculation. To make it even more unlikely, this reentry into the detection slice would need to be synchronized in time to cause a significant effect. (ii) In addition, T_1 relaxation is taking place during the recirculation time of about 4.5 s. For a perfect spin inversion by the selective pulse, a T_1 of blood of 1650 ms, and a recirculation time of 4.5 s, the longitudinal magnetization already has reached 87% of its thermal equilibrium value after the first recirculation. We

therefore believe that the recirculation of blood does not interfere with the slice-selective T_1 quantification.

To provide a quantitative estimation of the perfusion and the RBV, the measured T_1 values had to be connected with a tissue model. In our approach, tissue was described by the two-compartment model and several assumptions were necessary to end with Eqs. [1] and [3].

First, tissue was described as consisting of the intravascular capillary blood and the extravascular tissue. The arterial and venous systems were neglected. In addition, the theoretical biexponential relaxation was approximated by a monoexponential relaxation curve. This is reasonable since no distinct biexponential behavior was detectable in the data. Furthermore, "fast exchange" of water between the intracapillary and extravascular compartments through the capillary wall was assumed. Some results from other studies speak in favor of fast exchange in tissues such as the myocardium (12). The last assumption was a homogeneous blood–tissue partition coefficient of 0.95 mL/g in the myocardium.

However, with respect to the presence of "fast exchange" in the murine myocardium in the context of the presented method of quantification of the regional blood volume the following is to be noted.

In one of its aspects, Ref. (12) is directed to the determination of a lower limit of the exchange rate k_c between intra- and extracapillary space in the rat myocardium. In an illustrative way, the parameter $1/k_c$ can be considered to represent the mean time interval during which a spin is located within a capillary. Reference (12) provides that $k_c > 6.6$ 1/s ($k_c > 4.5$ 1/s with a probability of 95%) in the rat myocardium. Combining this result with Eq. [9] of Ref. (12) shows that the relationship between the spin-lattice relaxation rate of the myocardium and the spin-lattice relaxation rate of capillary blood is linear over a wide range.

Reference (40) is directed to the determination of the regional blood volume in the myocardium of humans using the similar technique. Accordingly, Eq. [1] of Ref. (40) corresponds to Eq. [9] of Ref. (12), whereby the exchange frequency f in (40) and the exchange rate k_c in (12) are interrelated via $f = \mathrm{RBV} \cdot k_c$. Figure 1 of Ref. (40) depicts the relationship according to Eq. [1]. Again, the relationship between the spin-lattice relaxation rate of the myocardium and the spin- lattice relaxation rate of capillary blood is linear over a wide range.

The presented method for determining the RBV according to Eq. [3] of the present paper holds, if the requirement of a linear relationship between the spin-lattice relaxation rate of the myocardium and the spin-lattice relaxation rate of capillary blood is fulfilled. From Fig. 1 of Ref. (40), it can be determined that the linear relationship holds up to a minimum spin-lattice relaxation time of capillary blood of about 300 ms (corresponding to a maximum spin-lattice relaxation rate of capillary blood of about 3 L/s in Fig. 1). Assuming that a relationship similar to that found in rats and humans holds for mice as well and taking into account that the relaxation times of capillary blood of mice determined in this study are much higher than the lower limit spin-lattice relaxation of capillary blood determined from Fig. 1 of Ref. (40) (mean values of 1847 ± 165 ms (1235 ± 261 ms) before (after) administration of the contrast agent determined in the present study), we believe that the presented technique for the quantification of the RBV can be applied even if "intermediate exchange" rather than fast exchange might be present in the murine myocardium.

It is noteworthy that the presented technique may easily be adapted for the analysis of other organs under the condition that the same tissue model can be applied for the selected organ.

In summary, the presented methods provide noninvasive in vivo quantification of the absolute perfusion and the regional blood volume in the murine myocardium for the first time. The results are in good agreement with values determined with the ex vivo microspheres technique and the method is sensitive enough to detect and visualize regional alterations of the perfusion after myocardial infarction.

With respect to the development of transgenic mouse models that show altered heart morphology, function, or metabolism, our technique may be an interesting tool for the noninvasive quantification of the myocardial microcirculation of the mouse in vivo.

ACKNOWLEDGMENTS

The authors thank Mark Griswold for very useful discussions, constant support, and his interest during the project. In addition, the authors gratefully acknowledge Sabine Voll and Carmen Bundschuh for their ambitious assistance and commitment during the project. Finally, the authors gratefully acknowledge Kai Hu for his performance of the surgical ligation of the LAD.

REFERENCES

1. Mural R, Adams E, Myers MD, et al. A comparison of whole-genome shotgunderived mouse chromosome 16 and the human genome. Science 2002;296:1661–1671.
2. Ruff J, Wiesmann F, Hiller K, Voll S, von Kienlin M, Bauer W, Rommel E, Neubauer S, Haase A. Magnetic resonance microimaging for noninvasive quantification of myocardial function and mass in the mouse. Magn Reson Med 1998;40:43–48.
3. Grupp I, Subramaniam A, Hewett T, Robbins J, Grupp G. Comparison of normal, hypodynamic and hyperdynamic mouse hearts using isolated work-performing heart preparations. Am J Physiol 1993;265:H1401–H1410.
4. Barbee R, Perry B, Ré R, Murgo J. Microsphere and dilution techniques for the determination of blood flows and volumes in conscious mice. Am J Physiol 1992;263:R728–R7332.
5. Trabold F, Pons S, Hagege A, Bloch-Faure M, Alhenc-Gelas F, Giudicelli J, Richer-Guidicelli C, Meneton P. Cardiovascular phenotypes of kinin B2 receptorand tissue kallikrein-deficient mice. Hypertension 2002;40:90–95.
6. Buckberg G, Luck J, Payne D, Hoffman J, Archie J, Fixler D. Some sources of error in measuring regional blood flow with radioactive microspheres. J Appl Physiol 1971;31:598–604.
7. Wilke N, Simm C, Zhang J, Ellermann J, Ya X, Merkle H, Path G, Ludemann H, Bache R, Ugurbil K. Contrast-enhanced first pass myocardial perfusion imaging: correlation between myocardial blood flow in dogs at rest and during hyperemia. Magn Reson Med 1993;29:485–497.
8. Jerosch-Herold M, Wilke N. Magnetic resonance quantification of the myocardial perfusion reserve with a fermi function model for constrained deconvolution. Med Phys 1998;25:73–84.
9. Kaji S, Ho H, Yang C, Quertermous T, Cooke J, Hu B. Quantitative analysis of first-pass magnetic resonance perfusion imaging of a mouse model of hindlimb ischemia (abstract). Proc Intl Soc Magn Reson Med; 71861:1999.

10. Bashir A, Bao J, Simons M, Post M, Burstein D. MR imaging of perfusion defects in mice (abstract). Proc Intl Soc Magn Reson Med 2000;8: 726.
11. Schwarzbauer C, Morissey S, Haase A. Quantitative magnetic resonance imaging of perfusion using magnetic labeling of water protons within the detection slice. Magn Reson Med 1996;35:540–546.
12. Bauer W, Roder F, Hiller K, Han H, Frohlich S, Rommel E, Haase A, Ertl G. The effect of perfusion on T1 after slice selective spin inversion in the isolated cardioplegique rat heart: measurement of a lower bound of intracapillary-extravascular water proton exchange rate. Magn Reson Med 1997;38:917–923.
13. Belle V, Kahler E, Waller C, Rommel E, Voll S, Hiller K, Bauer W, Haase A. In vivo quantitative mapping of cardiac perfusion in rats using a non invasive spin labeling method. J Magn Reson Imaging 1998;8:1240–1245.
14. Streif J, Hiller K, Waller C, Nahrendorf W, Wiesmann F, Bauer W, Rommel E, Haase A. In vivo assessment of absolute perfusion in the murine skeletal muscle with spin labeling MRI. J Magn Reson Imag 2003;17:147–152.
15. Bauer W, Hiller K, Galuppo P, Neubauer S, Köpke J, Haase A, Waller C, Ertl G. Fast high-resolution magnetic resonance imaging demonstrates fractality of myocardial perfusion in microscopic dimensions. Circ Res 2001;88:340–346.
16. Waller C, Kahler E, Hiller K, Hu K, Nahrendorf M, Voll S, Haase A, Ertl G, Bauer W. Myocardial perfusion and intracapillary blood volume in rats at rest and with coronary dilatation: MR imaging in vivo with use of a spin-labeling technique. Radiology 2000;215:189–197.
17. Kahler E, Waller C, Rommel E, Belle V, Hiller K, Voll S, Bauer W, Haase A. Perfusion-corrected mapping of cardiac regional blood volume in rats in vivo. Magn Reson Med 1999;42:500–506.
18. Bauer W, Hiller K, Roder F, Rommel E, Ertl G, Haase A. Magnetization exchange in capillaries by microcirculation affects diffusion-controlled spin-relaxation: a model which describes the effect of perfusion on relaxation enhancement by intravascular contrast agents. Magn Reson Med 1996;35:43–55.
19. Haase A. Snapshot FLASH MRI. Applications to T1, T2, and chemical-shift imaging. Magn Reson Med 1990;13:77–89.
20. Haacke E, Lenz G. Improving MR image quality in the presence of motion by using rephasing gradients. Am J Roentgenol 1987;148:1251–1258.
21. Krvitski N, Starostin D, Smith T. Extracorporal recording of mouse hemodynamic parameters by ultrasound velocity dilution. ASAIO J 1999;45:32–36.
22. Wiesmann F, Ruff J, Hiller K, Rommel E, Haase A, Neubauer S. Developmental changes of cardiac function and mass assessed with MRI in neonatal, juvenile and adult mice. Am J Physiol Heart Circ Physiol 2000;278:H652–H657.
23. Streif J, Lanz T, Griswold M, Rommel E, Haase A. A coil combination for magnetic resonance perfusion imaging of mice in vivo at 7 T. Rev Sci Instrum 2003;74:2843–2848.
24. Silver M, Joseph R, Hoult D. Highly selective Pi/2 and Pi pulse generation. J Magn Reson 1984;59:347–351.
25. Rommel E, Kuhstrebe J, Wiesmann F, Szimtenings M, Streif J, Haase A. A double trigger unit for ECG and breath triggered mouse heart imaging (abstract). Proceedings of the 17th Annual Meeting of the European Society for Magnetic Resonance in Medicine and Biology, 2000. p 568.
26. Ogan M, Schmiedl U, Moseley M, Grodd W, Paajanen H, Brasch R. Albumin labeled with Gd-DTPA: an intravascular contrast agent for magnetic resonance blood pool imaging: preparation and characterization. Invest Radiol 1987;22:665–671.
27. Deichmann R, Haase A. Quantification of T1 values by snapshot FLASH NMR imaging. J Magn Reson 1992;96:608–612.
28. Deetjen P. Wasser- und Elektrolythaushalt. In: Schmidt RF, Thews G, editors. Physiologie des Menschen 1990;24th ed. Berlin: Springer-Verlag; p 808–818.
29. Spindler M, Niebler R, Remkes H, Horn M, Lanz T, Neubauer S. Mitochondrial creatine kinase is critically necessary for normal myocardial high-energy phosphate metabolism. Am J Physiol Heart Circ Physiol 2002;283:H680–H687.
30. Crystal G, Czinn E, Silver J, Salem M. Coronary vasodilation by isoflurane abrupt versus gradual administration. Anesthesiology 1995;82: 542–549.
31. Ruff J, Wiesmann F, Hiller K, Neubauer S, Rommel E, Haase A. Influence of isoflurane anesthesia on contractility of the mouse heart in vivo. A NMR imaging study. Proc Eur Soc Magn Reson Med 1998;15: 169.
32. Dixon W, Brummer M, Malko J. Acquisition order and motional artifact reduction in spin warp images. Magn Reson Med 1988;6:74–83.
33. Roth D, Swaney J, Dalton N, Gilpin E, Ross J. Impact of anesthesia on cardiac function during echocardiography in mice. Am J Physiol Heart Circ Physiol 2002;282:H2134–H2140.
34. Decking U, Schrader J. Spatial heterogeneity of perfusion and energy turnover in the heart. Z Kardol 2001;90:970–977.
35. Waller C, Hiller K, Kahler E, Hu K, Nahrendorf M, Voll S, Haase A, Ertl G, Bauer W. Serial magnetic resonance imaging of microvascular remodeling in the infarcted rat heart. Circulation 2001;103:1564–1569.
36. Nahrendorf M, Hiller K, Hu K, Ertl G, Haase A, Bauer W. Cardiac magnetic resonance imaging in small animal models of human heart failure. Med Image Anal 2003;7:369–375.
37. Anversa P, Olivetti G, Capasso J. Cellular basis of ventricular remodeling after myocardial infarction. Am J Cardiol 1991;68:7D–16D.
38. Judd R, Levy B. Effects of barium induced cardiac contraction on large and small vessel intramyocardial blood volume. Circ Res 1991;68:217–225.
39. Crystal G, Downey H, Bashour F. Small vessel and total coronary blood volume during intracoronary adenosine. Am J Physiol 1981;241:H194–H201.
40. Wacker C, Wiesmann F, Bock M, Jakob P, Sandstede J, Lehning A, Ertl G, Schad L, Haase A, Bauer W. Determination of regional blood volume and intraextracapillary water exchange in human myocardium using Feruglose: first clinical results in patients with coronary artery disease. Magn Reson Med 2002;47:1013–1016.